ISSN 0016-7037
Volume 72, Number 16
August 15, 2008

Geochimica et Cosmochimica Acta

JOURNAL OF THE GEOCHEMICAL SOCIETY AND THE METEORITICAL SOCIETY

Volume 72, Number 16 August 15, 2008

Articles

Continued on outside back cover

Available online at www.sciencedirect.com
ScienceDirect
Geochimica et Cosmochimica Acta 72 (2008) 3929–3938
Geochimica et Cosmochimica Acta
www.elsevier.com/locate/gca

Dehydroxylation mechanisms in Al^{3+}/Fe^{3+} dioctahedral phyllosilicates by quantum mechanical methods with cluster models

Esther Molina-Montes [a], Vicente Timón [b], Alfonso Hernández-laguna [b], C. Ignacio Sainz-díaz [a,*]

[a] *Laboratorio de Estudios Cristalográficos, Instituto Andaluz de Ciencias de la Tierra, CSIC/Universidad de Granada, Av. Fuentenueva s/n, 18002 Granada, Spain*

[b] *Estación Experimental del Zaidín, Consejo Superior de Investigaciones Científicas (CSIC) C/Profesor Albareda 1, 18008 Granada, Spain*

Received 19 October 2007; accepted in revised form 21 April 2008; available online 21 June 2008

Abstract

Atomic models involving the dehydroxylation process of dioctahedral phyllosilicates without interlayer charge were used to calculate energies and explore the reaction paths of the possible mechanisms of this reaction at a quantum mechanical level. The geometrical features and electronic structure of a molecular cluster model of two edge-sharing octahedrally coordinated cations coupled to a ring of six silicate tetrahedra was evaluated by ab initio molecular orbital calculations with Hartree–Fock approximation. Two dehydroxylation mechanisms are considered. One mechanism involves two contiguous hydroxyl that are on an octahedron shared edge that joins a pair of octahedral cations. The other model considered involves OH loss from across an octahedral vacant. The substitution effect of Al^{3+} by Fe^{3+} in the octahedral sheet on the activation energy and structural transformations is compared by minimization of the critical points of the Potential Energy Surface (PES) for the reactant, transition state and product along the reaction path of the dehydroxylation process. The calculated energy differences and vibration frequencies are according to previous experimental results. The dehydroxylation mechanism involving OH across the octahedral hole, is less energetically favorable and is endothermic.

1. INTRODUCTION

The dehydroxylation of dioctahedral 2:1 phyllosilicates to the dehydroxylate derivative occurs over a broad range of temperature from 350 to 800 °C (Heller et al., 1962; Koster van Groos and Guggenheim, 1987; Drits et al., 1995). Dehydroxylation involves the formation and eventual elimination of one H_2O molecule per half unit cell from hydroxyl groups in the structure. Two possible dehydroxylation mechanisms have been proposed: one mechanism involves two adjacent (cis) hydroxyl groups on a shared edge between a pair of octahedral cations (Guggenheim et al., 1987) and another mechanism involves (trans) hydroxyl groups across the vacant octahedral site (Malhotra and Ogloza, 1989). Previous studies involving Nuclear Magnetic Resonance (NMR) (Fitzgerald et al., 1996), powder X-ray diffraction (XRD) (Wardle and Brindley, 1972), and infrared spectroscopy (Wang et al., 2002) of pyrophyllite and its dehydroxylate showed that the pyrophyllite dehydroxylate consists of five-coordinated, distorted, trigonal bipyramidal AlO_5 units in the former octahedral sheet, sandwiched between two distorted but intact tetrahedral SiO_4 sheets. A similar dehydroxylate structure occurs for muscovite (Udagawa et al., 1974). After H_2O molecule formation, a residual oxygen joins the two penta-coordinated Al atoms. Thermogravimetric studies of this reaction detected that the release of H_2O occurs in a two-step process (Guggenheim et al., 1987). Infrared spectroscopic studies of this process in pyrophyllite between

* Corresponding author. Fax: +34 958 181632.
E-mail address: cisainz@ugr.es (C.I. Sainz-díaz).

0016-7037/$ - see front matter © 2008 Elsevier Ltd. All rights reserved.
doi:10.1016/j.gca.2008.04.043

200 and 1500 °C revealed the formation of a structure intermediate during dehydroxylation with a new OH species exhibiting spectra at 3690 and 3702 cm^{-1}, but no structure was proposed (Wang et al., 2002). Previous rehydroxylation studies suggested that an intermediate should be formed during rehydroxylation of the dehydroxylate pyrophyllite, but no structure was proposed (Heller et al., 1962). Recently, Sainz-Díaz et al. (2004) found evidence for a semi-dehydroxylate derivative as an intermediate of this process by using quantum mechanical calculations with a good agreement with the spectroscopic studies of Wang et al. (2002). The complexity of the phyllosilicate samples, with low symmetry, heterogeneous chemical composition and high disorder-degree makes difficult to determine experimentally the different elementary steps and mechanisms of this process that have been reported. This can justify discrepancies in activation energy determination and mechanism proposals found in the literature (Gualtieri and Ferrari, 2006). One purpose of the present work is to study the mechanism and reaction path of the dehydroxylation process of dioctahedral trans-vacant phyllosilicates at the atomic scale.

On dehydroxylation of dioctahedral phyllosilicates, the main factor affecting the thermal stability of the octahedral sheet is the Al–OH bond strength (Guggenheim et al., 1987; Koster van Groos and Guggenheim, 1987). After the formation and release of the first H_2O, the remaining hydroxyl groups are bound more strongly to the cations, owing to the effect of the residual oxygen, which is undersaturated with respect to positive charge. Therefore, higher temperature is required for further H_2O release until complete dehydroxylation. Thus, the composition of the octahedral sheet also affects the thermal stability of the mineral. Infrared spectroscopy has shown that dehydroxylation is favoured when Mg and Fe octahedral cations are present (Heller-Kallai and Rozenson, 1980; Bray and Redfern, 2000) following the thermal stability sequence: Al–OH–Al > Al–OH–Mg > Fe–OH–Al > Fe–OH–Mg > Fe–OH–Fe.

Recently, Density Functional Theory (DFT) based calculations have been applied to the study of structural properties in phyllosilicates (Rosso et al., 2001; Sainz-Díaz et al., 2002, 2005; Botella et al., 2004; Hernández-Laguna et al., 2006) and dehydroxylation processes (Sainz-Díaz et al., 2004; Stackhouse et al., 2004) by using periodic crystal models. However, some points are still unclear, such as, the reaction paths, transition states and activation energy of dehydroxylation process. For studying these points theoretically at high level the use of clusters or molecular models can be useful. This approach is especially useful to study properties and reactions where local atomic environment is sufficient to describe the experimental phenomenon. Dehydroxylation of dioctahedral phyllosilicates involves the reactivity of the hydroxyl groups and can be considered as a phenomenon that is strongly dependent on a local atomic environment. Thus, with the choice of a correct cluster model, a good approximation can be made to describe the process. This approach allows determine the critical points of the Potential Energy Surface (PES) for the reaction path, including the transition states and then the reaction energy barrier can be determined. The transition state searching procedure has been widely used in molecules (Frisch et al., 1998). Since the cluster models are used as molecules, this transition state searching procedure is easily applied for clusters, whereas this procedure is more difficult to apply in periodic models.

Previous quantum mechanical studies on clusters or molecular models of silicates have been reported (Sauer et al., 1994; Lasaga, 1995), especially for the study of the OH properties in phyllosilicates (Kubicki and Apitz, 1998; Chatterjee et al., 2000; Sainz-Díaz et al., 2000; Timón et al., 2003), validating the utility of this approach. Here, we apply a similar methodology to the study of the dehydroxylation mechanism of dioctahedral phyllosilicates by finding an activation energy close to the experimental value. We also show the effect of cation substitution on reactivity. This paper summarizes the models of the structural transformation in dehydroxylation reaction, compares the energetics of the reaction depending on the octahedral composition, and provides a theoretical vibrational analysis of the possible models.

2. MODELS AND METHODS

The cluster model was selected to obtain the smallest local meaningful model. This model includes two octahedral cations with nearest-neighbor oxygen atoms so that two OH groups reside on a shared edge (Fig. 1). This cluster

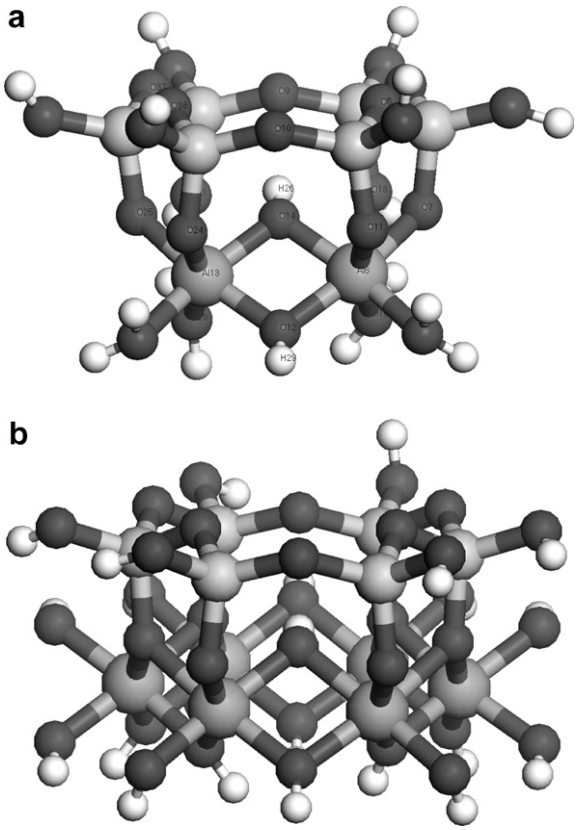

Fig. 1. Molecular cluster models $Si_6Al_2H_{16}O_{22}(OH)_2$ (a) and $Si_6Al_6H_{20}O_{38}(OH)_2$ (b). Si, Al, O and H atoms are represented by gray, dark gray, black and white colors, respectively.

was generated from the data of Wardle and Brindley (1972) for pyrophyllite [unit cell: Si_8 Al_4 O_{20} $(OH)_4$] by cutting a cluster of two complete octahedra, $[Al_2\ O_8\ (OH)_2]^{12-}$, and a ring of six SiO_4 tetrahedra. The dangling bonds were neutralized with hydrogen atoms ($Al_2Si_6O_{24}H_{18}$) (Fig. 1a). Thus, four terminal OH groups are formed within the same (M–OH–M′) plane and four terminal OH_2 groups are formed in association with the octahedral positions. This model is believed to contain the most relevant atoms to study the mechanism of the dehydroxylation in these minerals. This cluster was previously generated and optimized (Timón et al., 2003), and is superior and more realistic than smaller clusters simulating clays (Chatterjee et al., 2000; Sainz-Díaz et al., 2000), although it requires greater computational effort. The octahedral aluminum pair of this cluster model is substituted by one Fe^{3+} or by two Fe^{3+}, for determining the effect of substitutions of Fe^{3+}.

We use the Hartree–Fock (HF) approximation implemented in the Gaussian 98 (Frisch et al., 1998) program package. Dunning–Huzinaga full double zeta basis set (D95) including pseudopotentials and polarization functions (LANL2DZ) was used (Wadt and Hay, 1985). This approximation yielded good results of the effect of cation substitution on OH vibrational properties for similar clusters (Sainz-Díaz et al., 2000; Timón et al., 2003). Preliminary calculations with hybrid HF/DFT functionals yielded a significant deformation of the model that increased the difficulty of the study of this reaction. Nevertheless, we will perform comparative analysis between reactant and products and the electronic correlation effect will be minimized. All clusters were optimised by the Berny method (Schlegel, 1982). To study the reaction mechanisms and the effect of cation substitutions in octahedral sites, only the octahedral sheet was fully optimized whereas the tetrahedral sheet was fixed. The latter was not optimized because of its supposedly negligible contribution to the energy variations on the potential energy surface. In preliminary calculations, we tried to optimize this tetrahedral ring obtaining many local minima and the ring was partly deformed, because one part of this ring is not completed with the octahedra for maintaining the planarity of the ring as in phyllosilicates. Nevertheless, we tested to relax the whole ring with redundant coordinates during the optimization of the whole cluster and no improvement was observed, whereas the computational effort increased a lot and convergence problems appeared. We have to take into account that these clusters models are not real molecules, but models that represent fragments of solids where dangling bonds have been closed with hydrogen, resulting in some cases even water molecules close to the octahedral sheet model. The transition states were searching with the saddle point optimization procedure taking into account the eigenvelues of Hessian. The critical points of the PES along the reaction path were computed to obtain the default minimal forces threshold. For each critical point of the PES, the vibrational frequencies and Hessian eigenvalues were calculated; transition states were characterized to obtain the imaginary frequency. The Zero-point Energy (ZPE) was considered for all cases. No effect of the temperature is included, then our calculations will be static at 0 K.

We also studied different spin states for the Fe^{3+} models. Thus, we fixed several values of the spin multiplicity by comparing the relative energies of the optimized structures. For the $Fe^{3+}Fe^{3+}$ cluster, the triplet state was more stable than the singlet one. Thus, we considered the triplet state in our reactivity calculations.

Frequencies of the vibration modes were scaled by the standard factor of 0.89 to account for anharmonic effects, the neglect of electron correlation, and the limitations of the basis set (Pople et al., 1981; Gordon and Truhlar, 1986; Sauer et al., 1994; Lasaga, 1995; Kubicki and Apitz, 1998; Sainz-Díaz et al., 2000) before comparisons to experimental values.

The dehydroxylation mechanism that occurs via the vacant octahedral site (Malhotra and Ogloza, 1989) cannot be explored with this cluster model. Therefore, an extended cluster model was generated comprising a complete tetrahedral and octahedral sheet (Fig. 1b), with dangling bonds saturated with hydrogen atoms, as in the previous cluster model. For calculating this large model, the ONIOM (Maseras and Morokuma, 1995) approach implemented in Gaussian 98 was also used. Two ONIOM layers, the octahedral and the tetrahedral sheet, was defined and treated at ab initio (HF/lanl2dz) and semiempirical (PM3) quantum mechanical levels, respectively. The linking atoms between both sheets (the apical oxygens) were included into the ab initio layer, whereas the shared electrons were included in the semiempirical layer. The external OH bonds were fixed by redundant coordinates.

3. RESULTS

3.1. Reaction energy profile

Critical points of the reaction path for the cis-dehydroxylation mechanism (Guggenheim et al., 1987) (involving the two OH groups on the shared edge) are studied from pyrophyllite to the dehydroxylate that contains a H_2O molecule in the center of the ditrigonal cavity of the tetrahedral sheet. These critical points were optimized (Fig. 2). Our calculated energy barrier in the two Al^{3+} model is 55.04 kcal/mol for the H_2O formation, and this is consistent with a previous theoretical estimation of 56 kcal/mol in pyrophyllite (Stackhouse et al., 2004) and an experimental value of 60 kcal/mol in smectite (Bray and Redfern, 2000) and 46 kcal/mol in kaolinite (Bellotto et al., 1995). We propose here an energy barrier of the dehydroxylation reaction for the mechanism of the cis contiguous hydroxyl groups, but only for an isolated reaction path. Stackhouse et al. (2004) established that the activation energy of this reaction is independent of the dehydroxylation state of neighboring pairs. The activation energy is determined from the initial step of the dehydroxylation and it should not be affected by the prior loss of H atom elsewhere in the structure. Therefore, our calculations can represent one step of the actual dehydroxylation process within the cis mechanism, the first step for the semidehydroxylate formation or the second step for the dehydroxylate product formation.

We analyzed the effect of the substitution of Al^{3+} octahedral cations by either one Fe^{3+} substitution or by two Fe^{3+} cations, on the reaction energy. For the simultaneous $Fe^{3+}Fe^{3+}$ substitution, we take into account the most stable

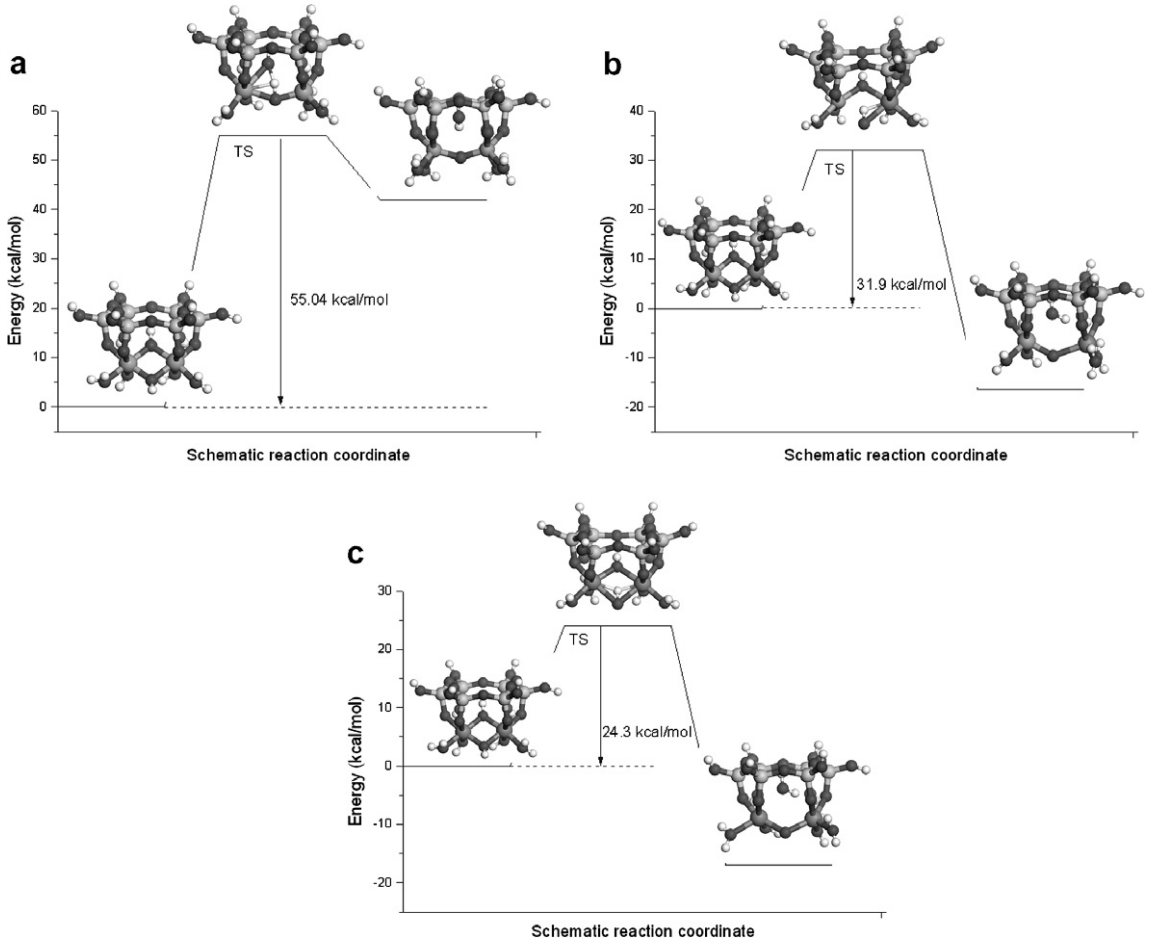

Fig. 2. Reaction path of the dehydroxylation reaction mechanism that occurs between two contiguous hydroxyl groups in $Si_6Al_2H_{16}O_{22}(OH)_2$ model of pyrophyllite (AlAl, a), with one Fe^{3+} substitution (AlFe, b) and with two Fe^{3+} substitutions (FeFe, c). Si, Al, O and H atoms are represented by gray, dark gray, black and white colors, respectively. The H atoms from bridging OH groups are represented by small gray spheres.

spin state, which is the high spin state (triplet), as previously established by Timón et al. (2003) in a smaller silicate cluster model. For other substitutions, the spin multiplicity was singlet ($Al^{3+}Al^{3+}$) and doublet ($Al^{3+}Fe^{3+}$). The substitution on the octahedral site changes the activation energy (Table 1) and hence the reaction rate, following the sequence: Fe^{3+}–OH–Fe^{3+} > Fe^{3+}–OH–Al^{3+} > Al^{3+}–OH–Al^{3+}. Thus, the FeFe pairs are the most favoured for dehydroxylation and the AlAl pair the less favoured one. This is consistent with the reactivity order postulated previously (Heller-Kallai and Rozenson, 1980; Bray and Redfern, 2000; Muller et al., 2000) based on infra-red spectroscopy studies of several phyllosilicates at high temperature. The structures of the critical points along the reaction coordinate are similar each other (Fig. 2) in all cases. Nevertheless, we observe some differences in the disposition of the H_2O molecule trapped in the ditrigonal cavity in the products of the substituted cluster models.

Table 1
Total energy (in Hartrees) of the calculated structures corrected with ZPE (in brackets) and comparison of energies ($\Delta E = E_{product} - E_{reactant}$ in kcal/mol) between critical points, and activation energy ($E_a = E_{TS} - E_{reactant}$ in kcal/mol) on the basis of octahedral composition

Substitution	Reactant	Transition state	E_a (kcal/mol)	Product
Al–OH–Al	−1834.5807002 (0.3275)	−1834.4929846	55.04 (0.3270)	−1834.5138864 (0.3292) $\Delta E = 41.9$
Al–OH–Fe	−1955.0204297	−1954.9695449 (0.3238)	31.93 (0.3256)	−1955.04669253 (0.3221) $\Delta E = -16.5$
Fe–OH–Fe	−2075.5051207 (0.3209)	−2075.4663882 (0.3239)	24.31	−2075.5321323 (0.3204) $\Delta E = -17.0$

In pyrophyllite, the determined energy for the product (dehydroxylate + H_2O) is less than the value for the reactant ($\Delta E = 41.9$ kcal/mol) and thus more stable, which is consistent with previous DFT calculations on pyrophyllite dehydroxylation [42.3 kcal/mol between pyrophyllite and product (dehydroxylate·H_2O + H_2O), Sainz-Díaz et al., 2004]. In contrast, in models with Fe^{3+} substitutions the product is more stable (≅16 kcal/mol) than the reactant.

3.2. Spectroscopic studies

Infrared spectroscopic studies of the dehydroxylation reaction for various phyllosilicates determined an estimate for the thermal stability of the M–OH bond and the rate of H_2O release (Heller-Kallai and Rozenson, 1980; Emmerich et al., 1999; Bray and Redfern, 2000; Muller et al., 2000). The frequency of the vibration modes of the OH groups showed notable differences with cation substitution. To verify the effects of these substitutions, we performed a vibrational analysis of the main vibration modes in reactants of the substituted clusters, and compared these results to the experimental determinations. The scaled calculated frequencies of the stretching, ν(OH), and bending in-plane, δ(OH), and out-plane, γ(OH), vibrations of the bridging OH groups are shown with experimental data in Table 2. The ν(OH) modes correspond only to the vibrational movements of these bridging OH groups without any contribution from the displacement of other atoms in the cluster. The δ(OH) modes of the bridging OH groups are distinguished easily but a small contribution from atomic displacements of the external O and H atoms occurs. However, the γ(OH) modes of these OH groups are difficult to determine owing to contributions from the external O and H atomic displacements.

A significant influence of the tetrahedral sheet on the ν(OH) frequency was observed in our calculations, owing to the non-bonding interactions between the hydrogen atom of the bridging OH group and the surrounding oxygen atoms of the tetrahedral sheet (Robert and Kodama, 1988; Sainz-Díaz et al., 2000). The ν(OH) frequency calculated for $O_{14}H_{26}$, that is oriented towards the tetrahedral ring, is slightly higher (3699 cm^{-1}) than the experimental value, 3675 cm^{-1} in pyrophyllite from Wang et al. (2002), and 3621 cm^{-1} in kaolinite from Johnston et al. (1985). This difference is related to an incomplete model that does not include either the another tetrahedral ring, representing the second tetrahedral sheet, nor the whole octahedral ring, representing the octahedral sheet, namely the hydroxyl groups associated with the octahedral vacancy. In phyllosilicates, hydroxyl groups are oriented to the tetrahedral sheet and surrounded by the structural oxygens of these tetrahedra. This atomic environment determines the local interaction of the hydroxyl groups. In our calculations, the ν(OH) frequency of the OH group that is oriented towards the zone without a tetrahedra ring, O_{12} H_{29} is 3725 cm^{-1} being close to the experimental value in gibbsite (3740 cm^{-1}, Saalfeld and Wedde, 1974), where there is no silicate tetrahedral sheet at all. This is also consistent with experimental value of ν(OH) frequency for OH groups non-oriented towards the tetrahedral sheet in kaolinite (3697 to 3669 cm^{-1}, Johnston et al., 1985). The ν(OH) frequency of O_{12} H_{29} is higher than that of the former one, $O_{14}H_{26}$, oriented towards the tetrahedra ring, owing to the lack of the non-bonding interactions with the tetrahedral oxygens. This effect was observed experimentally in kaolinite where ν(OH) band appears at 3620 and 3697 cm^{-1} for the OH groups oriented towards or not the tetrahedral sheet, respectively (Johnston et al., 1985). This result was not observed for the δ(OH) showing that this mode is less sensitive to the hydrogen bond interactions with the tetrahedral oxygens. In general, we find a good approximation to the experimental values, remarking the strong influence of the local atomic environment on the ν(OH) vibration frequencies.

Considering the reactivity of the bridging OH groups with cation substitution, the δ(OH) frequency (symmetric and antisymmetric modes) is found to decrease with the activation energy of the process (Fig. 3) following a linear relationship ($R = 0.9848$ and 0.9330 for symmetric and antisymmetric δ(OH) frequency, respectively) for the models substituted by Fe^{3+}. The decreasing of both, activation energy and δ(OH) frequency, indicates a weakening of the bonds involved in the process. Like in the experimental data, the octahedral composition determines the energy barrier of the reaction such that, Fe^{3+}-rich phyllosilicates, which contain a lower δ(OH) frequency, will dehydroxylate earlier than Al-rich phyllosilicates. However, the relationship between activation energy and ν(OH) frequency, related with the O–H bond strength, is not as linear as with δ(OH) frequency. Therefore, the reactivity of phyllosilicates in this reaction is related with the strength of the M–OH bond.

Table 2
Scaled theoretical vibration frequencies (in cm^{-1}) of phyllosilicate models compared to experimental values (in brackets)

Vibration mode	AlOHAl	AlOHFe	FeOHFe
ν(OH)	3725[a], 3699 (3740)[b], (3675)[c]	3701[a], 3684 (3573–3652)[d]	3703[a], 3695 (3535–3631)[d]
δ(OH)	947s, 968as (949)[c]	903s, 938as (890)[d,e]	873s, 898as (820)[f]
γ(OH)	418s, 431as (418, 482)[c]	441s, 452 as	430s, 478as
ν(Si–O)	1166 (1122)[c]	1160	1161
ν(Al–O)	630 (622)[g]	533	625

s, symmetric; as, antisymmetric.
[a] Bridging OH group without tetrahedral ring.
[b] In gibbsite (Saalfeld and Wedde, 1974).
[c] In pyrophyllite (Wang et al., 2002).
[d] In dioctahedral micas (Besson et al., 1987).
[e] In smectite, illite and pyrophyllite (Bray and Redfern, 2000).
[f] In montmorillonite (Vantelon et al., 2001).
[g] In montmorillonite (Emmerich et al., 1999).

3.3. Geometrical features

The main geometrical features of the calculated models for the cis mechanism (Guggenheim et al., 1987) are close to the experimental values (Table 3). Taking as reference the Al^{3+}–Al^{3+} cluster model, the O–H bond length of the hydroxyl group is similar in value (0.948 Å) to that in cluster

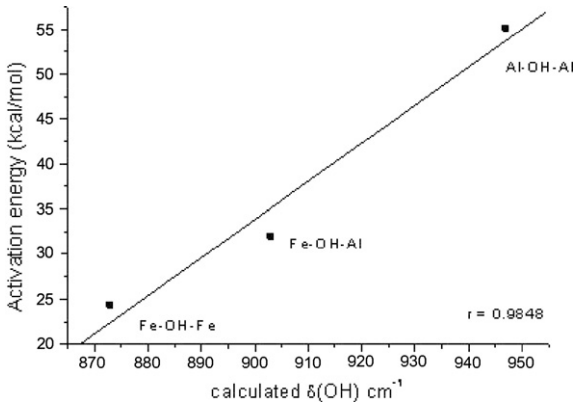

Fig. 3. Relationship between activation energy and δ(OH) frequency for the Fe^{3+} cation substitution effect.

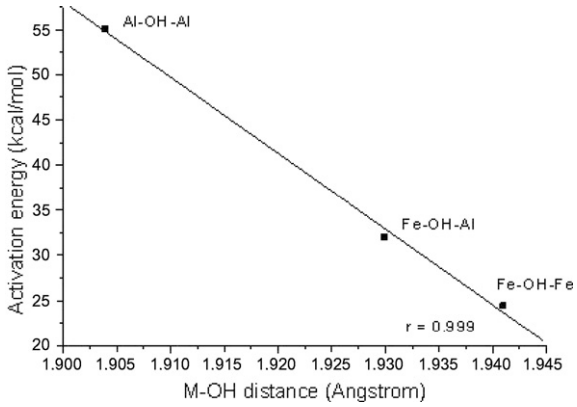

Fig. 4. Activation energy versus M–OH bond length (average values) for the Fe^{3+} cation substitution effect.

models of gibbsite (Kubicki and Apitz, 1998; Sainz-Díaz et al., 2000). However, the bridging OH group with an O–H vector pointing towards the tetrahedral ring has a slightly longer bond length (0.947 Å) than the former bridging OH group, owing to weak hydrogen-bond interactions between the H atom and the oxygen atoms of the SiO_4 groups. Thus, the strongest non-bonding interaction of this H atom is with the basal oxygen O_9 that is in front of the O–H bond with a distance (H...O) of 2.457 Å and angle (O–H...O = 142.8°). The non-bonding interactions between the OH group and the apical O atoms (O_{18} and O_{41}) are much weaker with longer H...O distances and smaller O–H...O angles. The interactions between the OH group and the other basal O atoms are very weak and they are thus weak electrostatic interactions. Because thermal stability is also attributed to the M–OH distance in relation with the vibrational frequency of the hydroxyl groups (Heller-Kallai and Rozenson, 1980), we also consider the average M–OH bond length with the activation energy (Fig. 4). The activation energy decreases with the increase in M–OH bond length following a linear relationship for isoelectric cation substitutions (Al^{3+} by Fe^{3+}). This suggests that the M–OH bond length is a factor in the energy-barrier height. Longer bond distances facilitate the release of the OH group and subsequent H_2O molecule

Table 3
Main geometrical features related with the bridging OH groups of the calculated clusters (distances in Å and angles in degrees)

Parameter	Reactant			Transition state			Product		
	Al–Al	Al–Fe	Fe–Fe	Al–Al	Al–Fe	Fe–Fe	AlAl	Al–Fe	Fe–Fe
d(M–M)	2.986 (2.97)[a]	3.005	3.028	3.499	3.315	3.343	3.315	3.805	3.589
d(M–OH)	1.904[c] (1.89)[a]	1.903_{Al}, 1.876_{Al}[b], 1.949_{Fe}, 1.968_{Fe}[b]	1.941[c]	2.01[c], 1.81[b,c]	1.92_{Al}, 2.22_{Al}[b], 2.07_{Fe}, 2.18_{Fe}[b]	2.02[c], 2.20[b,c]	1.761[b], 2.75_{H_2O}	1.90_{Al}[b], 2.27_{Fe}[b]	2.075[b,c], 2.750_{H_2O}[c]
d(O–H)	0.948, 0.947[b] (0.95)[d]	0.949 0.948[b]	0.953 0.952[b]	0.95, 1.06[b] $1.33_{H...O}$	0.95, 0.941[b] $1.61_{H...O}$	0.95, 0.943[b] $1.65_{H...O}$	0.952_{H_2O}	0.956_{H_2O}	0.955_{H_2O}
MOM	103.2 (100)[e]	102.6	100.3	87.6, 150.8[b]	112.2, 97.8[b]	110.8, 98.7[b]	140.3[b]	131.7[b]	119.9[b]
OMO	76.75 (80)[e]								
$d(H_{26}...O_9)$	2.457	2.462	2.598	2.261	2.297	2.296	2.205	2.249	2.352
$d(H_{26}...O_{41})$	3.135	3.145	3.433	2.997	3.055	3.092	3.560	3.269	3.465
$d(H_{26}...O_{18})$	3.208	3.231	3.321	3.108	3.086	3.134	3.626	3.442	3.592
$O_{14}H_{26}O_9$	142.8	141.1	128.0	114.9	177.9	178.3	108.7	122.6	107.8
$O_{14}H_{26}$ O_{18}	94.5	94.1	85.0	77.2	121.3	122.3			
$O_{14}H_{26}$ O_{41}	96.4	94.2	86.9	77.0	124.5	121.9			
v_i[f]				−1117	−1190	−1151			

Experimental values in brackets.
[a] From pyrophyllite and its dehydroxylate derivative (Lee and Guggenheim, 1981).
[b] Bridging OH located in the zone without tetrahedral ring that remains as residual bridging oxygen after dehydroxylation.
[c] Average value.
[d] Average value in muscovite (Catti et al., 1994).
[e] In gibbsite (Saalfeld and Wedde, 1974).
[f] Imaginary frequency of the transition vector in cm^{-1}.

formation. Thus, phyllosilicates with octahedral sheets containing Fe^{3+}–Fe^{3+} pairs show a lower activation energy for dehydroxylation than those with Al^{3+}–Al^{3+} pairs.

The dehydroxylation product maintains the geometry of the crystal lattice of the dehydroxylate derivative of pyrophyllite (Wardle and Brindley, 1972; Lee and Guggenheim, 1981). The fivefold coordination of Al (^{V}Al) in the dehydroxylate forms a trigonal bipyramid (Fitzgerald et al., 1996), where one oxygen atom bridges two ^{V}Al atoms, with one Al–O bond length of 1.76 Å, that is close to that reported experimentally (1.80 Å from Wardle and Brindley, 1972). This is drastically shorter than the Al–OH bond length of pyrophyllite of 1.90 Å (1.89 Å, Lee and Guggenheim, 1981). The AlOAl angle in the trigonal bipyramid is 140.3°, which is greater than in pyrophyllite but not near to the ideal value of 180°. In this product, the presence of the H_2O molecule in the ditrigonal cavity of tetrahedral sheet involves a repulsive interaction between O atoms. Therefore, the AlOAl angle does not reach the 180° value that is found in a dehydroxylated product and dehydrated derivative. This trigonal bipyramid produces also a significant enlargement of the M...M distance with respect to the reactants in all cases.

The trapping of the H_2O molecule in the ditrigonal cavity is controlled by hydrogen bond interactions of the H atoms with O atoms of the Si tetrahedra. One H atom is in the center of the tetrahedral ring and oriented in a perpendicular direction with respect to the basal (0 0 1) plane. This H atom (H_{26}) has a H bonding with the basal tetrahedral oxygen atom, O_9, and weaker interactions with the remaining of surrounding O atoms.

The transition state (TS) shows a structure close to the product. From the frequency analysis, this structure is a saddle point in the PES of the reaction. The frequencies of the transition vectors are similar for all TSs [(−1117)–(−1190) cm^{-1})]. By analyzing the eigenvalues of the Hessian, this structure proved to be a transition state of a reaction coordinate where the transition vector (ϕ) is defined mainly by the non-bonding (OH...OH) distance. The reaction involves the H atom of one OH group jumping to and bonding to another OH group. The result is the formation of a H_2O molecule and the residual O atom (Or). This reaction affects other geometrical features (O–Al bond length, HO...Or distance, bond angles and dihedral angles) [$\phi = 0.74\, d(\mathrm{Or...OH}) - 0.27\, d(\mathrm{HO...Or}) + 0.17 d(\mathrm{Al–OH}) + 0.29\, \theta(\mathrm{HO–Al–Si}) - 0.29\, \theta(\mathrm{Al–Or–OH}) + 0.23\, \theta(\mathrm{Or–Si–Al–Al}) - 0.22\, \theta(\mathrm{Or–Al–Si–O}) - 0.19\, \theta(\mathrm{H–O–Or–Al})$]. The variations of these geometrical parameters are similar for each TS. One OH group swings in accord with the out-of-plane bending vibration mode until it is oriented towards the other bridging O atom with a H...O distance of 1.54 Å. This situation forces the other O–H vectors to move away from the AlOHAl group towards the center of the hexagonal cavity. Then, the H atom bonds to the out-going OH group to generate a H_2O molecule. The octahedral cation substitutions do not change the transition vector configuration in TS and only slight geometrical variations are found, especially in the H...OH distance of the bridging OH groups. Larger H...O distances are associated with lower activation energies for the isoelectric cation substitutions (Al^{3+} by Fe^{3+}) with the reaction sequence order of:

$$\mathrm{Fe^{3+} - Fe^{3+}(H...O\ 1.65\ Å) > Al^{3+} - Fe^{3+}(H...O1.61\ Å) > Al^{3+} - Al^{3+}(H...O1.54\ Å)}$$

3.4. Charge

The lost of the OH group and H atom produces a local excess of positive charge that is distributed through the apical oxygen atoms, shortening the M–OH bond distance on the remaining hydroxyl groups. Therefore, a higher energy is required for the reaction progress as postulated by Guggenheim et al. (1987). Mulliken population analysis on the

Table 4
Mulliken atomic net charges of the calculated clusters

Atom	Reactant			Product		
	AlAl	AlFe	FeFe	AlAl	AlFe	FeFe
M–M	2.021^{Al}, 2.027^{Al}	2.072^{Al}, 1.419^{Fe}	1.465^{Fe}, 1.483^{Fe}	2.087^{Al}, 2.093^{Al}	2.092^{Al}, 1.285^{Fe}	1.237^{Fe}, 1.270^{Fe}
Si	2.26–2.33	2.26–2.33	2.28–2.34	2.28–2.34	2.27-2.34	2.29-2.35
O_{14}	−1.241	−1.156	−1.078	−0.930	−0.944	−0.930
H_{26}	0.501	0.494	0.486	0.510	0.493	0.502
O_{12}	−1.154	−1.079	−0.994	−1.415[a]	−0.693[a]	−0.624[a]
H_{29}	0.474	0.469	0.456	0.463	0.496	0.477
O_9	−1.229	−1.230	−1.230	−1.272	−1.262	−1.258
O_2	−1.180	−1.181	−1.182	−1.208	−1.203	−1.203
O_{37}	−1.187	−1.192	−1.192	−1.218	−1.213	−1.205
O_{41}	−1.069	−1.070	−1.081	−1.010	−1.051	−1.086
O_{18}	−1.063	−1.069	−1.069	−1.006	−0.999	−1.032
O_7	−1.276	−1.149	−1.151	−1.330	−1.292	−1.275
O_{11}	−1.268	−1.149	−1.149	−1.302	−1.266	−1.259
O_{24}	−1.297	−1.293	−1.161	−1.290	−1.282	−0.579
O_{25}	−1.285	−1.284	−1.169	−1.333	−1.321	−1.226

[a] Residual Or atom.

reactant and intermediate structures of the cluster allowed us to examine further this assumption quantitatively (Table 4). First, we affirm that the charge distribution of the apical oxygen atoms and residual oxygen atoms change along the reaction path, e.g. the residual oxygen O_{12} yields an undersaturation of positive charge and its net atomic charge is more negative (−1.15 in the reactant of Al–OH–Al to −1.42 in the intermediate of Al–Or–Al) and the net atomic charge of apical oxygen atoms increases slightly (−1.28 to −1.30 in the reactant, −1.29 to −1.33 in the intermediate of Al^{3+}–Al^{3+}). On the other hand, in the reactants, the negative net atomic charges of the oxygen atoms of the hydroxyl groups (O_{12} and O_{14}) with respect to the octahedral cation substitution show the following order: Al–OH–Al > Al–OH–Fe > Fe–OH–Fe. The charge distribution of both oxygen atoms shows linear relationships with the activation energy (Fig. 5), depending also on the octahedral cation composition. The octahedral composition and moreover the cation substitution in the octahedra determines the energetics of the dehydroxylation reaction.

3.5. Dehydroxylation mechanism across the octahedral hole

To investigate the dehydroxylation reaction mechanism involving the octahedral vacancy (hereafter referred to as the 'cross' mechanism) in pyrophyllite, the cluster model is extended to a complete octahedral ring including the hydroxyl groups of both parts of the octahedral vacancy. Dehydroxylation occurs between the hydroxyl groups that are oriented to the same octahedral hole. This model includes two coupled rings, one tetrahedral and one octahedral. Using ONIOM, we optimized the reactant and product structures as shown in Fig. 6. The energy of the reactant is 59.77 kcal/mol lower than that of the product. This energy difference is smaller (41.9 kcal/mol) in the other reaction mechanism involving contiguous hydroxyls. This result indicates that the activation energy of the cross mechanism is greater than in the mechanism involving contiguous hydroxyls (55 kcal/mol). In addition, the product of the cross mechanism is a semi-dehydroxylate intermediate of the cross reaction. Considering the results of Sainz-Díaz et al. (2004), the intermediate must have a lower energy than the final dehydroxylate product. Therefore, our results indicate that the cross mechanism is energetically less favoured than the mechanism involving contiguous hydroxyls. The migration effort of the H atom is much higher (longer distance) in this mechanism that in the previous one.

In the product, the H_2O molecule is stabilized by hydrogen bonds (1.557 and 2.128 Å) with the apical oxygens and by electrostatic interactions with the five-coordinated Al cations. These Al cations have an additional positive charge caused by the loss of one OH, which forms H_2O. An

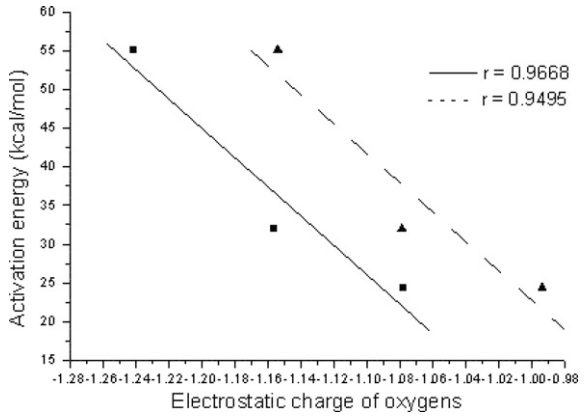

Fig. 5. Relationship between activation energy and Mulliken net atomic charge of the oxygens from OH groups for the Fe^{3+} cation substitution effect. Solid line is related to the O atom that forms water and dashed line is related to the residual O atom (Or).

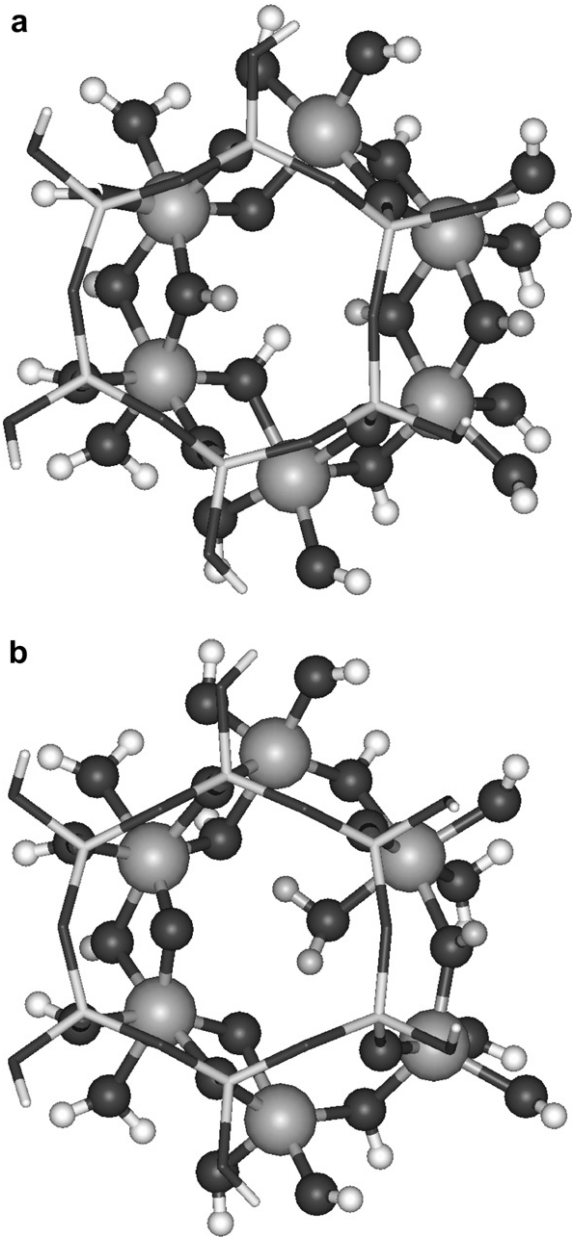

Fig. 6. Optimized structures of the reactant (a) and intermediate (b) in the dehydroxylation cross mechanism. Si, Al, O and H atoms are represented by gray, dark gray, black and white colors, respectively. The H atoms from bridging OH groups are represented by small gray spheres.

intermediate structure is formed with a pair of five-coordinated aluminum joined together with a remnant hydroxyl group OHr (Al–OHr–Al), whereas the remaining sixfold aluminum cations are joined by a residual oxygen atom (Al–Or–Al) and a hydroxyl group (Al–OH–Al). This intermediate structure is the starting point for a different reaction mechanism on both edges. Further research relating to this mechanism is forthcoming.

4. CONCLUSIONS

Our results suggest the usefulness of cluster models and the quantum–mechanical methodology for the study of phyllosilicate properties. The existence of a transition state along the on-site reaction path of dehydroxylation between the reactive and the product (dehydroxylate.H_2O) suggests that this path is one possible mechanism for dehydroxylation. The nature of this transition state indicates that the mechanism involves the breaking of two Al–O bonds forming a free OH group and the swing of the other H atom towards this free OH group to form H_2O. This mechanism is the same to that proposed by Guggenheim et al. (1987). The energy difference between reactive and product in our cluster models is similar to that found in real crystal lattice models (Sainz-Díaz et al., 2004). The reaction barrier found (55.04 kcal/mol) is consistent with the activation barrier found experimentally for the dehydroxylation of smectite (59.8 kcal/mol, Bray and Redfern, 2000) and kaolinite (46 kcal/mol, Bellotto et al., 1995).

The dehydroxylation mechanism of Malhotra and Ogloza (1989), where the H atom migrates through the octahedral vacant site to join to the vicinal OH group (cross mechanism), was examined by the ONIOM model cluster approach. We conclude that the cross mechanism is energetically less favoured than the mechanism proposed by Guggenheim et al. (1987).

The substitution of octahedral Fe^{3+} cations causes variations in the M–OH bond lengths and vibration frequencies of the OH groups that are linearly related with activation energy. The Fe^{3+} substitution increases significantly the reactivity of the OH groups for the dehydroxylation reaction, and the reaction follows the sequence: Fe–Fe > Al–Fe > Al–Al, according to experimental observations.

Although our models represent likely the structure of pyrophyllite or kaolinite with different degrees of Fe substitution, the results of this work can be applied qualitatively for other dioctahedral phyllosilicates, since the limiting step is the formation of H_2O.

ACKNOWLEDGMENTS

The authors thank S. Guggenheim for his fruitful reviewing and the "Centro Técnico de Informática" of CSIC, Centro de Cálculo del CIEMAT, CESGA, and the "Centro de Supercomputación de la Universidad de Granada" for allowing the use of computational facilities. E. Molina-Montes thanks MEC (FPU Program) and CSIC (I3P Program) for financial support. This work was supported by Spanish MCYT and European FEDER Grants BTE2002-03838, CGL2005-02681/BTE and CTQ2004-04648.

REFERENCES

Bellotto M., Gualtieri A. F., Artioli G. and Clark S. M. (1995) Kinetic study of the kaolinite–mullite reaction sequence. I. Kaolinite dehydroxylation. *Phys. Chem. Miner.* **22**, 207–214.

Besson G., Drits V. A., Daynyak L. G. and Smoliar B. B. (1987) Analysis of cation distribution in dioctahedral micaceous minerals on the basis of IR spectroscopy data. *Clay Miner.* **22**, 465–478.

Botella V., Timón V., Escamilla-Roa E., Hernández-Laguna A. and Sainz-Díaz C. I. (2004) Hydrogen bonding and vibrational properties of hydroxy groups in the crystal lattice of dioctahedral clay minerals by means of first principles calculations. *Phys. Chem. Miner.* **31**, 475–486.

Bray H. J. and Redfern S. A. T. (2000) Influence of counterion species on the dehydroxylation of Ca^{2+}, Mg^{2+}, Na^{+} and K^{+}—exchanged Wyoming montmorillonite. *Mineral. Mag.* **64**, 337–346.

Catti M., Ferraris G., Hull S. and Pavese A. (1994) Powder neutron diffraction study of 2MI muscovie at room pressure and at 2 GPa. *Eur. J. Mineral* **6**, 171–178.

Chatterjee A., Iwasaki T. and Ebina T. (2000) A novel method to correlate layer charge and the catalytic activity of 2:1 dioctahedral smectite clays in terms of binding the interlayer cation surrounded by monohydrate. *J. Phys. Chem.* **104**, 8216–8223.

Drits V. A., Besson G. and Muller F. (1995) An improved model for structural transformations of heat-treated aluminous dioctahedral 2:1 layer silicates. *Clays Clay Miner.* **43**, 718–731.

Emmerich K., Madsen F. T. and Kahr G. (1999) Dehydroxylation behavior of heat-treated and steam-treated homoionic cis-vacant montmorillonites. *Clays Clay Miner.* **47**, 591–604.

Fitzgerald J. J., Hamza A. I., Dec S. F. and Bronnimann C. E. (1996) Solid-state silicon-29 and aluminium-27 nuclear magnetic resonance investigation of the dehydroxylation of pyrophyllite. *J. Phys. Chem.* **88**, 6206–6209.

Frisch M. J., Trucks G. W., Schlegel H. B., Scuseria G. E., Robb M. A., Chesseman J. R., Zarzewki V. G., Montgomery J. A., Stratmann R. E., Burant J. C., Dapprich S., Millam J. M., Daniels A. D., Kudin K. N., Strain M. C., Farkas O., Tomasi J., Barone V., Cossi M., Cammi R., Mennucci B., Pomelli C., Adamo C., Clifford S., Ochterski J., Petersson G. A., Ayala P. Y., Cui Q., Morokuma K., Malick D. K., Rabuck A. D., Raghavachari K., Foresman J. B., Cioslowski J., Ortiz J. V., Stefanov B. B., Liu G., Liashenko A., Piskorz P., Komaromi I., Gomperts R., Martin R. L., Fox D. J., Keith T. A., Al-Laham M. A., Peng C. Y., Nanayakkara A., Gonzalez C., Challacombe M., Gill P. M. W., Johnson B. G., Chen W., Wong M. W., Andres J. L., Head-Gordon M., Replogle E. S. and Pople J. A. (1998) Gaussian 98, rev. A.7. Gaussian, Inc., Pittsburgh, PA.

Gordon M. S. and Truhlar D. G. (1986) Scaling all correlation energy in perturbation theory calculations. *J. Am. Chem. Soc.* **108**, 5412–5419.

Gualtieri A. F. and Ferrari S. (2006) Kinetics of illite dehydroxylation. *Phys. Chem. Miner.* **33**, 490–501.

Guggenheim S., Chang Y.-H. and Koster van Gross A. F. (1987) Muscovite dehydroxylation: high-temperature studies. *Am. Mineral.* **72**, 537–550.

Heller L., Farmer V. C., Mackenzie R. C., Mitchell B. D. and Taylor H. F. W. (1962) The dehydroxylation and rehydroxylation of triphormic dioctahedral clay minerals. *Clay Miner. Bull.* **5**, 56–72.

Heller-Kallai L. and Rozenson I. (1980) Dehydroxylation of dioctahedral phyllosilicates. *Clays Clay Miner.* **28**, 355–368.

Hernández-Laguna A., Escamilla-Roa E. and Sainz-Díaz C. I. (2006) DFT study of the cation arrangements in the octahedral

and tetrahedral sheets of dioctahedral 2:1 phyllosilicates. *Phys. Chem. Miner.* **33**, 655–666.

Johnston C. T., Sposito G. and Birge R. R. (1985) Raman spectroscopic study of kaolinite in aqueous suspension. *Clays Clay Miner.* **33**, 483–489.

Koster van Groos A. F. and Guggenheim S. (1987) High-pressure differential thermal analysis (HP-DTA) of the dehydroxylation of Na-rich montmorillonites and K-exchanged montmorillonite. *Am. Mineral.* **72**, 1170–1175.

Kubicki J. D. and Apitz S. E. (1998) Molecular cluster models of aluminium oxide and aluminium hydroxide surfaces. *Am. Mineral.* **83**, 1054–1066.

Lasaga A. C. (1995) Fundamental approaches in describing mineral dissolution and precipitation rates. In *Chemical Weathering Rates of Silicate Minerals*, vol. 31 (eds. A. F. White and S. L. Brantley), pp. 23–86. Reviews in Mineralogy. Mineralogical Society of America, Washington, DC.

Lee J. H. and Guggenheim S. (1981) Single crystal X-ray refinement of pyrophyllite-1Tc. *Am. Mineral.* **66**, 350–357.

Malhotra V. M. and Ogloza A. A. (1989) FTIR spectra of hydroxyls and dehydroxylation kinetics mechanism in montmorillonite. *Phys. Chem. Miner.* **16**, 386–393.

Maseras F. and Morokuma K. (1995) IMOMM: a new integrated ab initio + molecular mechanics geometry optimization scheme of equilibrium structures and transition states. *J. Comput. Chem.* **16**, 1170–1179.

Muller F., Drits V. A., Plancon A. and Robert J. L. (2000) Structural transformation of 2:1 dioctahedral layer silicates during dehydroxylation–rehydroxylation reactions. *Clays Clay Miner.* **48**, 375–381.

Pople J. A., Schlegel H. B., Krishnan R., DeFrees D. J., Binkley J. S., Frisch M. J., Whiteside R. A., Hout R. J. and Hehre W. J. (1981) Molecular orbital studies of vibrational frequencies. *Int. J. Quant. Chem., Quant. Chem. Symp.* **15**, 269–280.

Robert J-L. and Kodama H. (1988) Generalization of the correlation between hydroxyl-stretching wavenumbers and composition of micas in the system K_2OM_2O–Al_2O_3–SiO_2–H_2O: a single model for trioctahedral and dioctahedral micas. *Am. J. Sci.* **288A**, 196–212.

Rosso K. M., Rustad J. R. and Bylaska E. J. (2001) The exchange in muscovita interlayer: an ab initio treatment. *Clays Clay Miner.* **49**, 500–513.

Saalfeld H. and Wedde M. (1974) Refinement of the crystal structure of gibbsite. *Z. Kristallogr. Kristallgeom. Kristallphys. Kristallchem.* **139**, 129.

Sainz-Díaz C. I., Timón V., Botella V. and Hernández-Laguna A. (2000) Isomorphous substitution effect on the vibration frequencies of hydroxyl groups in molecular cluster models of the clay octahedral sheet. *Am. Mineral.* **85**, 1038–1045.

Sainz-Díaz C. I., Timón V., Botella V., Artacho E. and Hernández-Laguna A. (2002) Quantum mechanical calculations of dioctahedral 2:1 phyllosilicates: effect of octahedral cation distribution in pyrophyllite, illite, and smectite. *Am. Mineral.* **87**, 958–965.

Sainz-Díaz C. I., Escamilla-Roa E. and Hernández-Laguna A. (2004) Pyrophyllite dehydroxylation process by First-Principles calculations. *Am. Mineral.* **89**, 1092–1100.

Sainz-Díaz C. I., Escamilla-Roa E. and Hernández-Laguna A. (2005) Quantum mechanical calculations of trans-vacant and cis-vacant polymorphism in dioctahedral 2:1 phyllosilicates. *Am. Mineral.* **90**, 1827–1834.

Sauer J., Ugliengo P., Garrone E. and Saunders V. R. (1994) Theoretical study of van der Waals complexes at surface sites in comparison with the experiment. *Chem. Rev.* **94**, 2095–2160.

Schlegel H. B. (1982) Optimization of equilibrium geometries and transition structures. *J. Comput. Chem.* **3**, 214–218.

Stackhouse S., Coveney P. V. and Benoit D. M. (2004) Density-Functional-Theory based study of the dehydroxylation behaviour of aluminous dioctahedral 2:1 layer-type clay minerals. *J. Phys. Chem.* **B108**, 9685–9694.

Timón V., Sainz-Díaz C. I., Botella V. and Hernández-Laguna A. (2003) Isomorphous cation substitution in dioctahedral 2:1 phyllosilicates by means of ab initio quantum mechanical calculations on clusters. *Am. Mineral.* **88**, 1788–1795.

Udagawa S., Urabe K. and Hasu H. (1974) The crystal structure of muscovite dehydroxylate. *Jpn. Assoc. Mineral. Petrol. Econ. Geol.* **69**, 381–389.

Vantelon D., Pelletier M., Michot L. J., Barres O. and Thomas F. (2001) Fe, Mg and Al distribution in the octahedral sheet of montmorillonites. An infrared study in the OH-bending region. *Clay Miner.* **36**, 369–379.

Wadt W. R. and Hay J. (1985) Ab initio effective core potentials for molecular calculations. *J. Chem. Phys.* **82**, 284–298.

Wang L., Zhang M., Redfern S. A. T. and Zhang Z. (2002) Dehydroxylation and transformation of the 2:1 phyllosilicate pyrophyllite at elevated temperatures: an infrared spectroscopic study. *Clays Clay Miner.* **50**, 272–283.

Wardle R. and Brindley G. W. (1972) The crystal structures of pyrophyllite, 1Tc, and its dehydroxylate. *Am. Mineral.* **57**, 732–750.

Associate editor: James R. Rustad